

IN SILICO MOLECULAR MODELING OF SALICYL HYDRAZONE ANALOGUES AS TROPOMYOSIN KINASE (TRKA) INHIBITORS**Ranjana, Neetu Sharma, Ajeet Singh* and A. K. Srivastava**

QSAR Laboratory, Department of Chemistry, University of Allahabad, Allahabad-211002, India.

Article Received on
19 July 2017,

Revised on 08 August 2017,
Accepted on 29 August 2017

DOI: 10.20959/wjpr201710-9499

Corresponding Author*Ajeet Singh**

QSAR Laboratory,
Department of Chemistry,
University of Allahabad,
Allahabad-211002, India.

ABSTRACT

The quantitative structure activity relationship between molecular structure and biological activity of salicyl - hydrazone analogues has been studied to explore the inherent factors affecting their biological activity. In the present analysis, quantum chemical parameters based on density functional theory, Topological descriptors were calculated at GGA-PW91 level of theory. In this Quantitative structure-activity relationships (QSAR) study, stepwise linear regression (MLR) analysis was used to select significant molecular descriptors. Based on selected descriptors, the significant QSAR models were constructed. The calculated regression models suggest that the presence of hydroxyl

group OH at R₁ position enhances the activity and showed better cytotoxicity. Model equations were cross-validated by leave one out (LOO) technique. Based on statistically significant model obtained in the present QSAR analysis, pIC₅₀ value was calculated for new tropomyosin kinase (TrkA) inhibitors.

KEYWORDS: salicyl-hydrazone, QSAR, cytotoxicity, TrkA inhibitor.

INTRODUCTION: Cancer is among the world's leading causes of death and is a major public health concern. Despite recent advances in cancer patients relapse particularly for cancers of brain, pancreas and late stage lung cancer so, there is an urgent need to develop new classes of chemotherapeutic agents to treat cancer that demonstrate pronounced and selective cytotoxicity against human cancer cell lines. Tropomyosin-receptor-kinases are a family of transmembrane receptors with a key role in function and survival of the neurons in the central nervous system. Trks function is complex, their activation inducing many intracellular changes that regulate neuronal plasticity, neuronal regeneration and apoptosis,

both *in vitro* and *in vivo*. Disregulation of Trks function has frequently been observed in neurodegenerative diseases, such as Alzheimer's and Parkinson's diseases. Trks are also involved in cancer biology. Trks alterations were found in several human neoplasms: neuroblastoma, medulloblastoma, glioblastoma, prostate cancer, pancreatic carcinoma. For this reason, many pharmacological strategies have been developed to inactivate TRKs or to suppress their expression in several diseases and disorders. Receptor tyrosine kinases (RTK) regulate critical cellular processes, such as cell proliferation, metabolism, and migration. Deregulation of RTKs has been reported in various types of cancer, and RTK-targeted therapies, such as inhibition of epidermal growth factor receptor (EGFR) in NSCLC, have been successfully developed.^[1]

NTRK1-3 gene family encodes tropomyosin receptor kinases (TrkA, B, and C), which are activated by neurotrophins. Nerve growth factor, brain-derived neurotrophic factor (BDNF), and neurotrophin-3 bind to TrkA, TrkB, and TrkC, respectively. On ligand binding, the tyrosine kinase and its downstream signaling are activated. Members of the Trk family are highly expressed in cells of neural origin, and are involved in neural maintenance and development.^[2]

Although functions related to neural cells have been extensively examined, the Trk receptor was originally described as an oncogene. Oncogenic Trk was reported as a fusion gene between the 5' region of the tropomyosin and the tyrosine kinase domain of TrkA derived from Inv (1q) inversion. The fused protein resulted in constitutive activation of the tyrosine kinase. This type of constitutively active TrkA fusions were reported in a subset of papillary thyroid cancers and colon cancers.^[3,4]

Overexpression of TrkB has been reported in several malignancies, such as neuroblastoma,^[5] prostate cancer, pancreatic ductal adenocarcinoma,^[6] multiple myeloma,^[7] and lung cancer.^[8] High levels of TrkB correlate with poor outcome.^[9] *In vitro*, TrkB has been shown to be involved in cancer cell proliferation, anoikis, cell migration/invasion, and epithelial-mesenchymal transition.^[10,11] These results suggest that TrkB may have a significant impact on the malignant phenotype of tumors *in vivo*. Accumulating evidence suggests that TrkB is a potential target for cancer therapy. Several small molecules that inhibit Trk signaling have been developed recently and are being tested in phase I and phase II trials.^[12]

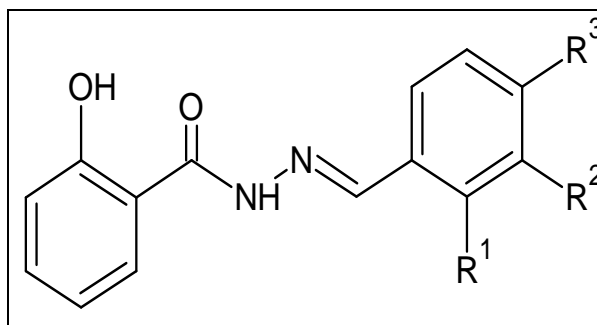
Theoretical background

Two dimensional (2D) structures of various derivatives of substituted pyridinone derivatives were drawn using ACD Lab Chem Sketch version 12.0 software (www.acdlabs.com/acdlabs-rss-feed.xml) and physicochemical and hydrophobic parameter such as formula weight (Fw), molecular weight (Mw), molecular volume (Mv), molar refractivity (Mr), parachor (Pc), index of refraction (IOR), surface tension (st), density (D), polarizability (Pz) and partition coefficient (Log P) were calculated with the help of this software. The topological parameters such as balaban indices (JX and JY), Wiener index (W), Bonding information content (BIC), molecular connectivity (χ) and 3D structures of compounds were also drawn on Accelrys's Discovery Studio 3.5 program. We have calculated quantum chemical descriptors^[8] such as: total energy (TE), Binding or cohesive Energy (BE), Band gap (BG), Softness (S), hardness (η) and chemical potential (μ), Electrophilic index (ω) Dipole moment (Di), highest occupied molecular orbital energy (HOMO), lowest unoccupied molecular orbital energy (LUMO) and most negative valued point (V_{\min}) in gas phase at GGA/PW91 level of theory.

The statistically significant models were evaluated by examining the regression coefficient, the standard deviation, the cross validation leave-one out statistics^[9] and the proportion between the cases and variables in the equation.^[10] We have used Hansch analysis for developing the models.^[11-17] Structural details of compounds with their experimental activity ($\log IC_{50}$) with indicator parameters are given in table 1.

Table 1: Structural detail and biological activity for series of salicyl - hydrazone analogues with indicator parameter.

Sr. no.	R ₁	R ₂	R ₃	I ₁	pIC ₅₀ ^A
1	H	H	H	0	5.2262
2	H	H	Cl	0	5.0074
3	H	H	NO ₂	0	5.0555
4	NO ₂	H	H	0	4.7075
5	H	H	NMe ₂	0	4.7323
6	H	H	CH ₃	0	5.0083
7	H	H	OH	0	5.0409
8	H	H	OCH ₃	0	4.8428
9	OH	H	OH	1	6.0604
10	OCH ₃	H	OCH ₃	0	4.8380
11	H	OH	OH	0	5.0390
12	OH	OH	OH	1	5.7077



RESULTS

QSAR studies were performed on a set of 12 compounds of salicyl-hydrazone analogues. On the basis of diversity between different substituent and reported biological activities, this series of compounds have been selected for QSAR analysis. In this series tropomyosin receptor kinase inhibitory activity has been expressed as IC_{50} reported by Yuanyuan Cao *et al.* (2015) in micro-molar (μM) units which were converted to their log units ($\log IC_{50}$) and used in the present investigation. This was done in order to reduce skewness of the data set. IC_{50} represents the concentration of drug that inhibits 50% of Trks(tropomyosin receptor kinase enzyme). The value of physicochemical, topological and quantum chemical parameters, which are used for making various significant models, are given in Table 2 and 3. Statistically significant models were obtained when some of these parameters were combined with the indicator parameter.

Table 2: Physicochemical and Topological descriptor for the present series of compound.

Sl. no.	Fw	Mr	Mv	Pc	Ior	St.	Den	Pz	Logp	A Logp	Log D	Ior	Dipole	χ^0	χ^1	χ^2	χ^3	J _x	J _y	W
1	240.257	69.77	204.9	536.1	1.596	46.8	1.17	27.66	3.71	2.441	2.406	1.596	2.0133	12.7947	8.7708	7.3378	0.8116	1.9516	2.0312	702
2	274.702	74.38	214.2	565.0	1.610	48.3	1.28	29.48	4.46	3.105	3.70	1.610	2.0120	13.6649	9.1647	7.9596	1.1002	1.93997	2.0252	826
3	299.281	80.04	226.4	620.2	1.625	56.3	1.32	31.73	3.24	2.486	2.451	1.625	2.3254	15.9494	10.5585	9.3500	1.4239	1.8880	1.9851	1297
4	299.281	80.04	226.4	620.2	1.625	56.3	1.32	31.73	3.24	2.486	2.45	1.625	1.5979	15.9494	10.5754	9.2679	1.3490	2.0046	2.1113	1201
5	297.351	86.47	257.0	664.2	1.587	44.5	1.15	34.28	4.65	3.122	3.073	1.587	3.0055	15.7862	10.7027	8.8627	1.0157	1.8636	1.9372	1316
6	254.283	74.20	220.1	567.2	1.588	44.0	1.15	29.41	4.17	2.927	2.892	1.588	2.1718	13.6649	9.1647	7.9596	1.1002	1.9507	2.025	826
7	256.256	70.63	202.2	541.8	1.615	51.4	1.26	28.00	3.08	2.199	2.163	1.615	2.7166	13.6649	9.1647	7.9596	1.1002	1.9417	2.0287	826
8	270.283	75.59	226.6	586.4	1.581	44.7	1.19	29.96	3.57	2.425	1.389	1.581	1.8374	14.372	9.7027	8.1287	1.0157	1.9178	2.0101	969
9	272.256	71.48	199.5	547.4	1.635	56.6	1.36	28.33	4.25	1.957	1.902	1.635	3.2929	14.5352	9.5753	8.4893	1.2985	1.9910	2.0906	930
10	300.309	81.40	248.3	636.6	1.569	43.1	1.20	32.27	3.18	2.408	2.373	1.569	2.5758	15.9494	10.6514	8.8495	1.1449	2.0078	2.1246	1208
11	272.256	71.48	199.5	547.4	1.635	56.6	1.36	28.33	2.83	1.957	1.904	1.635	2.6042	14.5352	9.5753	8.4674	1.2830	1.9713	2.0690	941
12	288.255	72.33	196.8	553.1	1.656	62.3	1.46	28.67	4.13	1.715	1.669	1.656	3.2998	15.4054	10.0029	8.8667	1.3947	2.0314	2.1428	1048

Table 3: DFT based descriptor for the present series of compound.

Sl. no.	TE	BE	HOMO	LUMO	BGE	Hardness(η)	Softness(s)	Che.pot(μ)
1	-800.68	-5.8449	-0.2034	-0.1020	0.1014	0.0507	19.7238	-0.1527
2	-1260.3	-5.8153	-0.2064	-0.1079	0.0985	0.0493	20.2839	-0.1572
3	-1036.22	-7.4877	-0.2134	-0.1256	0.0877	0.0439	22.7790	-0.1699
4	-1036.21	-7.4874	-0.2114	-0.1324	0.0789	0.0395	25.3164	-0.1719
5	-956.91	-8.4331	-0.1786	-0.0921	0.0864	0.0432	23.1213	-0.1353
6	-833.06	-7.0418	-0.2037	-0.1054	0.0982	0.0491	20.3458	-0.1545
7	-868.84	-6.7263	-0.1993	-0.1024	0.0968	0.0484	20.6398	-0.1508
8	-907.78	-7.2421	-0.1971	-0.1015	0.0955	0.0478	20.9205	-0.1493
9	-943.59	-6.9459	-0.1940	-0.0991	0.0948	0.0474	21.0748	-0.1465
10	-1021.47	-7.9786	-0.1940	-0.0976	0.0928	0.0464	21.5517	-0.144
11	-943.58	-6.9352	-0.1973	-0.1024	0.0949	0.0474	21.0970	-0.1498
12	-1018.33	-7.1571	-0.1941	-0.0984	0.0957	0.0478	20.8986	-0.1462

In multiple regression analysis, the independent variables must be orthogonal. To check the orthogonality, we have performed autocorrelation and the descriptors correlation matrix is given in table 4 & 5. Statistically significant multi parametric models were obtained when one of the parameters (Fw), (logP) (D), (Bic), (Mw), (Mr), (Di), HOMO, (μ), (ω) and LUMO is combined with the indicator parameter. The various statistical significant models were obtained and shown below.

Table 4: Correlation matrix between different physicochemical and topological parameters of cancer cell line SK-OV-3(Act1).

	pIC ₅₀	Mv	Pc	Pz	X0	X1	Wiener	I ₃
pIC ₅₀	1.000							
MV	-.676	1.000						
PC	-.593	.943	1.000					
PZ	-.584	.938	.995	1.000				
X0	-.185	.558	.780	.763	1.000			
X1	-.307	.690	.875	.858	.983	1.000		
Wiener	-.324	.703	.891	.883	.963	.986	1.000	
I ₃	.910	-.484	-.348	-.337	.119	-.008	-.050	1.000

Table 5: Correlation matrix between different DFT parameters of cancer cell line SK-OV-3(Act1).

	PIC ₅₀	BGE	HOMO	LUMO	TE	I ₃
PIC ₅₀	1.000					
BGE	.388	1.000				
HOMO	-.316	-.750	1.000			
LUMO	.275	.584	-.674	1.000		
TE	.086	.270	-.165	.298	1.000	
I ₃	.910	.133	-.119	.271	-.046	1.000

Modeling of pIC₅₀ using empirical parameter

$$\text{pIC}_{50} = 0.00627 (\pm 0.011) \text{ mv}$$

$$+ 0.781 (\pm 500.939) I_1 - 6.334$$

$$n=12, R=0.949, R^2=0.900, R^2_A=0.878, S.E=0.1397, F_{(2,9)}=40.515, Q=6.793 \dots\dots\dots(1)$$

Eq. 1 explains only 90.0 % variance in the TrkA inhibitory activity. It shows that descriptor with higher molar volume(mv) contribute positively.

$$\text{pIC}_{50} = -0.00294 (\pm 0.0004) \text{ Pc}$$

$$+ 0.822 (0.483) I_1 - 6.678$$

$$n=12, R=0.956, R^2=0.915, R^2_A=0.896, S.E=0.1291, F_{(2,9)}=48.160, Q=7.4051 \dots\dots\dots(2)$$

$$\text{pIC}_{50} = -0.0606 (\pm 0.091) \text{ Pz}$$

$$+ 0.826 (\pm 0.48) I_1$$

$$n=12, R=0.956, R^2=0.915, R^2_A=0.896, S.E=0.12961, F_{(2,9)}=48.160, Q=7.4051 \dots\dots\dots(3)$$

Equation 2 and Equation 3 explains 91.5% variance in the TrkA inhibitory activity. the descriptors parachor (Pc) and polarizability (Pz) both have negative sign while coefficient of indicator parameter I_1 (OH grp) has positive sign it shows that hydroxyl group contributes positively and enhances the value of pIC₅₀

Modeling of pIC₅₀ using quantum chemical parameters

$$\text{pIC}_{50} = 17.30 (\pm 30.688) \text{ BGE}$$

$$+ 0.897 (\pm 0.494) I_1 + 3.332$$

$$n=12, R=0.949, R^2=0.900, R^2_A=0.872, S.E=0.1394, F_{(2,9)}=40.660, Q=6.8077 \dots\dots\dots(4)$$

Eq. 4 explains only 90.1 % variance in the TrkA inhibitory activity. It shows that descriptor Band gap energy (BGE) and indicator parameter I_1 contribute positively towards the activity of drugs. It is the best equation obtained using quantum chemical descriptor.

$$\text{pIC}_{50} = -0.711 (\pm 1.835) \text{ HOMO}$$

$$+ 0.908 (\pm 0.559) I_1 - 4.838$$

$$n=12, R=0.934, R^2=0.872, R^2_A=0.843, S.E=0.1583, F_{(2,9)}=30.548, Q=5.9001 \dots\dots\dots(5)$$

$$\text{pIC}_{50} = 1.025 (\pm 22.102) \text{ LUMO}$$

$$+ 0.926 (\pm 0.666) I_1 + 5.059$$

$$n=12, R=0.910, R^2=0.829, R^2_A=0.790, S.E=0.1829, F_{(2,9)}=21.752, Q=4.9753 \dots\dots\dots(6)$$

Equation 5 explains only 87.2% variance and Equation 6 explains 82.9 % in the TrkA inhibitory activity. It shows that HOMO contributes negatively and LUMO contributes the group presented by I_1 contribute positively in both the equations.

$$\begin{aligned}
 & \text{pIC}_{50} = 0.00042 (\pm 0.002) \text{ TE} \\
 & \quad + 0.940 (\pm 0.612) I_1 + 5.359 \\
 & n=12, R=0.919, R^2=0.844, R_A^2=0.810, \text{S.E.}=0.1744, F_{(2,9)} = 24.379, Q = 5.2694 \dots (7) \\
 & \text{pIC}_{50} = -0.175 (\pm 0.253) \chi^1 \\
 & \quad + 0.932 (\pm 0.445) I_1 + 6.668 \\
 & n = 12, R = 0.958, R^2 = 0.918, R_A^2 = 0.899, \text{S.E.} = 0.1269, F_{(2,9)} = 50.065, Q = 7.549 \dots (8) \\
 & \text{pIC}_{50} = -0.108 (\pm 0.16) \chi^0 \\
 & \quad + 0.971 (\pm 0.455) I_1 + 6.528 \\
 & n = 12, R = 0.957, R^2 = 0.915, R_A^2 = 0.896, \text{S.E.} = 0.12889, F_{(2,9)} = 48.391, Q = 7.4249 \dots (9) \\
 & \text{pIC}_{50} = 0.0005 (\pm 0.001) w \\
 & \quad + 0.920 (\pm 0.476) I_1 + 5.511 \\
 & n = 12, R = 0.952, R^2 = 0.906, R_A^2 = 0.885, \text{S.E.} = 0.1355, F_{(2,9)} = 43.310, Q = 7.0222 \dots (10)
 \end{aligned}$$

Equation 7 explains only 84.4% variance in the TrkA inhibitory activity. It shows that Total energy (TE) contribute positively. It is the best equation obtained using quantum chemical descriptor.

Where;

n = Number of compounds in the data set

R = Correlation coefficient

R^2 = Coefficient of determination

R_A^2 = Adjusted coefficient of determination

S.E. = Standard error of estimate

F = Variance ratio

Q = Quality of fit

Each equation (1 to 3) is a representative of one model for QSAR. The above equations shows that the steric parameter molar volume (m_v) is positive this shows that substituent with higher molar volume is preferred and enhances the inhibitory activity, while the other two steric parameters parachor (P_c) and polarizability (P_z) is negative. In all the three models (eqn1, 2 and 3) there is a positive sign of coefficient of indicator I_1 (OH) it shows that hydroxyl group should be retained at R_1 for future drug designing.

The equation 4-10 shows that the lowest unoccupied molecular orbital energy (LUMO), band gap energy (BGE), total energy (TE) and weiner index (w) have positive effect on the

inhibitory activity. while highest unoccupied molecular orbital HOMO , zero order molecular connectivity index χ^0 and first order molecular connectivity of χ_1 is negative this shows that substituent with less branching is preferred for influencing the Trka inhibition activity. The positive sign of coefficients of indicators I_1 indicates hydroxyl group (OH) at at R_1 position contribute positively towards the activity of drugs. In all the above equations, R , R^2 and R^2_A are substantially high and SE is fairly low, indicating that these models are statistically significant in all the statistical terms.

QSAR studies depend on development of models, validation of models and utility of developed model. The validation of model is essential part of QSAR analysis.^[18] All the multi-parametric models were found to be statistically significant based on F_{test} . F_{test} values are given in equations.

Out of several QSAR model, model 2, 8 and 9 show best result. In order to confirm that the model with excellent statistics has also excellent prediction power too, we have evaluated quality factor Q . The predictive power as determined by the Pogliani $Q^{[19-20]}$ parameter for the model expressed by eq.2 [$Q = 7.4051$], eq.8 [$Q = 7.549$] and for eq.9 [$Q = 7.4249$], confirms that these models have excellent statistics as well as excellent predictive power.

According to equation 2,8 & 9 compound having lower value of parachor ,lower value of zero order molecular connectivity and first order molecular connectivity and presence of hydroxyl group at R_1 position is favorable for Inhibition of Trka enzyme more potentially.

Predicted and residual activity values for model (2, 8& 9) are given in Table 6. Predicted values are the calculated activities obtained from model (2, 8 & 9) and the residual values are the difference between the observed biological activities and calculated activities The plot of observed pIC_{50} verses predicted pIC_{50} for equation (2, and 8) is shown in graph (figure 1, and 2) and the predicted R^2 was found to be fairly large.

Table 6: Comparison between observed and predicted activities of model 8 and model 2.

Observed activity	Predicted activity	Residual	Predicted activity	Residual
5.2262	5.1306	.0955	5.1036	.1225
5.0074	5.0616	-.0542	5.0188	-.0114
5.0555	4.8174	.2380	4.8567	.1987
4.7075	4.8144	-.1069	4.8567	-.1492
4.7323	4.7921	-.0598	4.7275	.0047
5.0083	5.0616	-.0533	5.0123	-.0040

5.0409	5.0616	-.0207	5.0869	-.0460
4.8428	4.9673	-.1245	4.9559	-.1131
6.0604	5.9215	.1388	5.8924	.1679
4.8380	4.8011	.0368	4.8085	.0294
5.0390	4.9897	.0492	5.0704	-.0314
5.7077	5.8465	-.1388	5.8756	-.1679

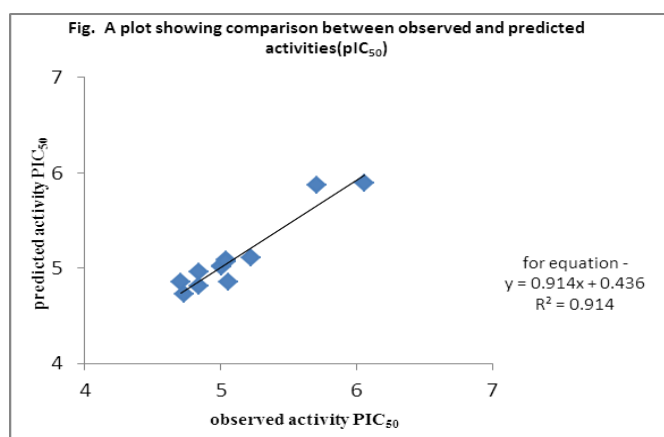


Fig. 1: A plot showing comparison between observed and predicted activities (pIC₅₀) for model 2.

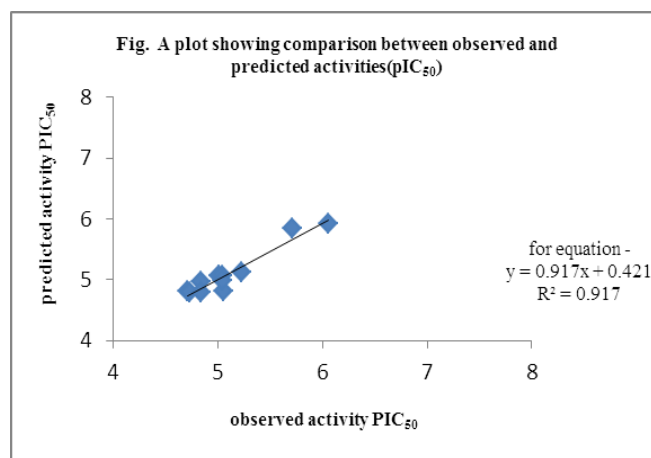


Fig. 2: A plot showing comparison between observed and predicted activities(pIC₅₀) for model 8.

Cross validation

The cross validation analysis was performed using leave one out (LOO) method,^[21-22] in which one compound is removed from the data set and the activity is correlated using the rest of the data set. The cross-validated R^2 in each case was found to be very close to the value of R^2 for the entire data set and hence these models can be termed as statistically significant. Cross validation provides the values of PRESS, SSY, PSE, R^2_{CV} and R^2_A from which we can

test the predictive power of the proposed model. These statistical parameters can be calculated from following equations:

$$\text{PRESS} = \sum (X_{\text{obs}} - X_{\text{cal}})^2 \dots\dots\dots \text{(i)}$$

$$\text{SSY} = \sum (X_{\text{obs}} - X_{\text{mean}})^2 \dots\dots\dots \text{(ii)}$$

$$S_{\text{PRESS}} = \sqrt{\text{PRESS}/n} \dots\dots\dots \text{(iii)}$$

$$r_{\text{cv}}^2 = 1 - \frac{\text{PRESS}}{\text{SSY}} \dots\dots\dots \text{(iv)}$$

$$r_{\text{adj}}^2 = 1 - (r^2) \left(\frac{n-1}{n-p-1} \right) \dots\dots\dots \text{(v)}$$

Where, X_{obs} , X_{cal} , and X_{mean} are observed, calculated, and mean values; n , number of compound in data set; p , number of independent parameters.

PRESS value validates a regression model with regards to predictability. To calculate PRESS, each observation is individually omitted. The $N-1$ observations are used to calculate a regression and estimate the value of omitted observation. This exercise is done in time, once for each observation. Smaller the PRESS values better the predictability of the model. If the value of SSY is less than that of PRESS the model would be better than chance and can be considered statically significant. The PRESS value is useful for deriving the r_{cv}^2 statics, call r^2 cross validated, which reflects the prediction ability of the model. In other word the approach of different statics that are derived by r_{cv}^2 has characteristic feature because of we can validate a regression mode without selecting another sample or splitting your data. A fair chance will be with data that r^2 is very high and r_{cv}^2 is very low, such data reviled that the fitted model is data dependent. r_{cv}^2 value may vary from zero to one. If r_{cv}^2 value beyond to this range, it is truncated to stay within this range. In such cases the adjusted r-squared (r_{adj}^2) play an important role and remove the distortion due to a small sample size.

In number of cases r_{cv}^2 and r_{adj}^2 is taken as a proof of the high predicative models. The statistical characteristic which have larger than that of 0.5 is consider as proof of the high predictive ability of the model. Our predicted models have higher value than that of 0.5. However, for practical purposes of end users the use of square root of PRESS/n , which is called predictive square error (PSE), is more directly related to the uncertainty of the predictions. The PSE values also support our results (Table7). The calculated cross-validated parameters confirm the validity of the models.^[22-23]

Table 7: Cross validated parameters and predictive error of coefficient of correlation (PE) for proposed models.

Sr. No.	Model	N	R	1 -R ²	PE	6PE	Press	SSY	Press/SSY	R ² CV	PSE
1	A+mv+I ₁	12	.949	0.1	0.0192	0.1152	.176	1.582	0.1112	0.8888	0.0146
2	A+pc+I ₁	12	.956	0.085	0.0163	0.0978	.150	1.607	0.0933	0.9067	0.0125
3	A+pz+I ₁	12	.956	0.085	0.0163	0.0978	.150	1.607	0.0933	0.9067	0.0125
4	A+Bge+I ₁	12	.949	0.100	0.019	0.1152	.176	1.582	0.1112	0.8888	0.0146
5	A+Homo+I ₁	12	.934	0.128	0.0246	0.1476	.226	1.532	0.1475	0.8525	0.0188
6	A+Lumo+I ₁	12	.910	0.171	0.0329	0.1974	.301	1.456	0.2067	0.7933	0.0250
7	A+TE+I ₁	12	.919	0.156	0.0222	0.1332	.274	1.484	0.1846	0.8154	0.0228
8	A+ χ^1 +I ₁	12	.958	0.082	0.0157	0.0942	.145	1.613	0.0898	0.9102	0.0120
9	A+ χ^0 +I ₃	12	.957	0.085	0.0163	0.0978	.150	1.608	0.0932	0.9068	0.0125
10	A+ w+I ₃	12	.952	0.094	0.0180	0.108	.165	1.592	0.1036	0.8964	0.0137

The predictive error (PE)^[21] of coefficient of correlation is yet another parameter used to decide the predictive power of the proposed models.^[24-27] We have calculated PE value of all the proposed models and the values are reported in Table 7. It is worth mentioning that if the values $R < PE$, then such correlation is not significant; however if values are $R > PE$ in several times (at least three times), then values are correlated. However, if values are $R > 6PE$, then mathematically the correlation is unquestionably good.

Our calculated results follow the condition $R > 6PE$ and it infer that our model have good predictive power. Calculated result also reviled that for future drug designing in this series, substituent should have more branching.

CONCLUSION

From the calculated QSAR model, the positive coefficients of molar volume (mv), DFT descriptors band gap energy (BE), lowest unoccupied molecular orbital (LUMO), total energy (TE) and topological descriptor weiner index (w) indicate that they have a positive effect on the inhibitory activity. The positive sign of coefficients of indicator I₁ shows that the hydroxyl group has a positive influence on activity and should be used at R₁ position in the future drug designing. The negative sign of coefficients of HOMO, parachor (Pc), polarizability (Pz) and molecular connectivity zero order χ^0 , and molecular connectivity first order χ^1 , has a negative influence on activity towards Trka enzyme of the compound. In all the models (eqn1 to eqn 10) the coefficient of indicator parameter I₁ is there at R₁ position contribute positively towards the activity of drugs. In all the above equations, R, R² and R²_A are substantially high and SE is fairly low, indicating that these models are statistically significant in all the statistical terms. The negative value of value of χ^0 and χ^1 suggest that the

substituent with less branching should be preferred for future modeling of Trka inhibition. The positive sign of coefficients of indicator I_1 shows that the OH group has positive influence on activity and should be used at R_1 position in the future drug designing of similar series of compound.

ACKNOWLEDGEMENT

Author A.K. Srivastava thanks University Grants Commission, New Delhi, India, for financial support. A. Singh wise to acknowledges UGC, New Delhi, India, for Dr. D. S. Kothari postdoctoral fellowship.

REFERENCES

1. Martin-Zanca D, Hughes SH, Barbacid M (April). "A human oncogene formed by the fusion of truncated tropomyosin and protein tyrosine kinase sequences". *Nature*, 1986; 319(6056): 743–8.
2. "Entrez Gene: NTRK1 neurotrophic tyrosine kinase, receptor, type 1".
3. Benito-Gutiérrez E, Garcia-Fernández J, Comella JX (February). "Origin and evolution of the Trk family of neurotrophic receptors". *Mol. Cell. Neurosci*, 2006; 31(2): 179–92.
4. Lambiase A, Merlo D, Mollinari C, Bonini P, Rinaldi AM, D' Amato M, Micera A, Coassin M, Rama P, Bonini S, Garaci E (November). "Molecular basis for keratoconus: lack of TrkA expression and its transcriptional repression by Sp3". *Proc. Natl. Acad. Sci. U.S.A.*, 2005; 102(46): 16795–800.
5. Vaishnavi, Aria; Capelletti, Marzia; Le, Anh T.; Kako, Severine; Butaney, Mohit; Ercan, Dalia; Mahale, Sakshi; Davies, Kurtis D.; Aisner, Dara L. (11-01). "Oncogenic and drug-sensitive NTRK1 rearrangements in lung cancer". *Nature Medicine*, 2013; 19(11): 1469–1472.
6. Yu T, Calvo L, Anta B, López-Benito S, Southon E, Chao MV, Tessarollo L, Arévalo JC (April). "Regulation of trafficking of activated TrkA is critical for NGF-mediated functions". *Traffic*, 2011; 12(4): 521–34.
7. Koch A, Mancini A, Stefan M, Niedenthal R, Niemann H, Tamura T (March). "Direct interaction of nerve growth factor receptor, TrkA, with non-receptor tyrosine kinase, c-Abl, through the activation loop". *FEBS Lett*, 2000; 469(1): 72–6.
8. Yano H, Cong F, Birge RB, Goff SP, Chao MV (February). "Association of the Abl tyrosine kinase with the Trk nerve growth factor receptor". *J. Neurosci. Res.*, 2000; 59(3): 356–64.

9. Acd-Lab software for calculating the referred physicochemical parameters. Chem Sketch www.acdlabs.com/acdlabs-rss-feed.xml.
10. Perdew JP, Wang Y .Accurate and simple density functional for the electronic exchange energy: Generalized gradient approximation. *Phys. Rev. B.*, 1986; 33: 8800–8802.
11. Perdew J P, Wang Y Accurate and simple analytic representation of the electron-gas correlation energy. *Phys. Rev. B.*, 1992; 45: 13244.
12. Mullera K, Altmannb R, Prinza H 2-Arylalkyl-substituted anthracenones as inhibitors of 12-lipoxygenase enzymes. 1. Structure–activity relationships of the terminal aryl ring. *Eur. J. Med. Chem.*, 2001; 36: 569.
13. Cramer III, R D, Bunce, J D, Patterson, D E, Frank, I E Cross validation, Bootstrapping, and partial least squares compared with multiple regression in conventional QSAR studies. *Quant. Struct. Act. Relat.*, 1988; 7: 18.
14. Hansch C, Leo A Exploring QSAR – Fundamentally and Application in Chemistry and Biology. *Amer. Chem. Soc.*, Washington, DC, 1995.
15. Hanch C, Fujita T p- σ - π Analysis A method for the correlation of biological activity and chemical structure. *J. Am. Chem. Soc.*, 1969; 86: 1616.
16. Srivastava A. K., Pathak V K., Jaiswal A, Agarwal, V Kc QSAR analysis of Mur B inhibitors with antibacterial properties discussing role of physico-chemical parameters. *Med. Chem. Res.*, 2011; 20: 1713.
17. Srivastava A K., Shukla N, Pandey A, Srivastava A., QSAR based modeling on a series of α -hydroxy amides as a novel class of bradykinin B1 selective antagonists. *J. Saudi. Chem. Soc.*, 2011; 15: 215.
18. Srivastava A K., Shukla N QSAR based modeling on a series of lactam fused chroman derivatives as selective 5-HT transporters. *J. Saudi. Chem. Soc.*, 2012; 16: 405.
19. Srivastava A K., Shukla N Quantitative structure activity relationship (QSAR) studies on a series of imidazole derivatives as novel ORL1 receptor antagonists. *J. Saudi. Chem. Soc.*, 2013; 17: 321.
20. Srivastava A K, Jaiswal M, Archana S, Chaurasia S, QSAR of substituted N-benzyl piperidines in the GBR series. *J. Ind. Chem. Soc.*, 2008; 85; 842.
21. Pogliani L. Structural property relationships of amine acids and some Peptides. *Amino acids*, 1994; 6: 141.
22. Pogliani L. Modeling with special descriptors derived from a medium size set of connectivity indices. *J. Phys. Chem*, 1996; 100: 18065.

23. Cramer III R D, Bunce J D, Patterson D.E., Frank I.E Cross validation, Bootstrapping, and partial least squares compared with multiple regressions in conventional QSAR studies. *Quant. Struct. Act. Relat*, 1988; 7: 18.
24. Chatterjee S, Hadi A S, Price B *Regression Analysis by Example*, 3rd Edn. Wiley VCH, New York, 2000.
25. Diudea M V *QSPR/QSAR studies for molecular descriptors*. Ed, Nova Science, and Huntington, New York, 2001.
26. Bikash D, Shovanlal G, Subrata B, Soma S, Jha, T QSAR study on some pyridoacridine ascididiamine analogues as antitumor agents. *Bioorg. Med. Chem*, 2003; 11(24): 5493.
27. Leonard JT, Roy K on Selection of Training and Test Sets for the Development of Predictive QSAR models. *QSAR & Combinatorial Science*, 2006; 25: 235.
28. Dwivedi A, Srivastava A K., Singh A Quantitative structure–activity relationship based modeling of substituted indole Schiff bases as inhibitor of COX-2. *J. Saudi*, 2013.
29. Dwivedi A, Srivastava A K., Singh A, Molecular Modeling of Pyridine Derivatives for COX-2 Inhibitors: Quantitative Structure Activity Relationship Study. *Med. Chem*, 2013.